

Dodecylresorufin (C12R) outperforms resorufin in micro-droplet bacterial assays

Ott Scheler^{†‡}, Tomasz S. Kaminski[†], Artur Ruszczak[†] and Piotr Garstecki^{†*}

[†]Institute of Physical Chemistry, Polish Academy of Sciences, Kasprzaka 44/52, 01-224 Warsaw, Poland.

[‡]Institute of Molecular and Cell Biology, University of Tartu, Riia 23 51010, Tartu, Estonia

ABSTRACT: This paper proves that dodecylresorufin (C12R) outperforms resorufin (the conventional form of this dye) in droplet microfluidic bacterial assays. Resorufin is a marker dye that is widely used in different fields of microbiology and has increasingly been applied in droplet microfluidic assays and experiments. The main concern associated with resorufin in droplet-based systems is the dye leakage into oil phase and neighboring droplets. The leakage decreases the performance of assays as it causes averaging of the signal between the positive (bacteria containing) and the negative (empty) droplets. Here we show that C12R is a promising alternative to conventional resorufin as it maintains higher sensitivity, specificity and signal-to-noise (SNR) ratio over time. These characteristics make C12R a suitable reagent for droplet digital assays and for monitoring microbial growth in droplets. Keywords: droplet microfluidics, bacteria viability assay, resorufin, dodecylresorufin, droplet emulsion

INTRODUCTION

Here, we demonstrate that dodecylresorufin (C12R) is an attractive alternative to resorufin as a metabolic marker of bacteria that are encapsulated in micro-droplets. C12R exhibits less leakage between the droplets. This in turn provides for higher stability of the fluorescent signal over time, increased signal to noise ratio and better accuracy of the assay in terms of increased true-positive and true-negative rates, as compared to the same assays executed with resorufin.

Droplet microfluidics has increasingly been demonstrated as a suitable tool in diverse applications in microbiology, including: i) detection¹⁻³ and identification^{4,5} of bacteria, ii) antibiotic susceptibility studies with endpoint measurement,^{1,3,6,7} iii) continuous monitoring of growth,⁸⁻¹⁰ iv) studies of interactions between microbial communities,¹¹⁻¹³ and v) high-throughput screening of novel molecules^{14,15} or of microbial cells for traits of interest.^{16,17} The main advantages of droplet microfluidics over conventional techniques include faster detection and the ability to carry out single-cell and high-throughput analysis.

Usually, in resorufin-based assays in microbiology, substrates presenting low intensity of fluorescence are converted to highly fluorescent resorufin by bacterial metabolism or by specific enzymes. Three different substrates have been described so far in droplet-based assays. One of such substrates is resazurin that is also the main component in AlamarBlue® and PrestoBlue® viability assays. Aerobic organisms metabolically convert (reduce) resazurin to fluorescent resorufin. The dye has therefore been widely used as an universal viability indicator.¹⁸⁻²² The exact mechanism of reduction is not known, whether it occurs intracellularly via enzyme activity or in the

medium as chemical reaction. Several reductase enzymes have been linked, but not fully confirmed being responsible for conversion.²³

Resazurin-based assays have also been combined with droplet microfluidics in antibiotic susceptibility studies.^{1,7,8} Secondly, the resorufin can be complexed with fluorescence-quenching component, allowing for the release of the dye by specific bacterial enzymes as demonstrated in droplet digital platform for bacterial enumeration² and in enzymatic kinetic analysis.²⁴⁻²⁶ Third popular substrate in droplet resorufin assays is the Amplex® Red reagent. It is converted to resorufin in a two-step process. Specific microbial oxidase enzymes produce hydrogen peroxide which promotes the conversion of the substrate to resorufin by peroxidase – an enzyme added to the reaction.²⁷⁻³⁰ Amplex® Red reagent has been used in droplet assays to measure enzymatic activity²⁹ and in high-throughput screening of microbes for metabolic production^{27,28} or consumption²⁸ of specific substrates.

In all of the assays mentioned above, the detectable product is resorufin. Unfortunately, there is a significant challenge in maintaining stable concentration of resorufin in droplets as the dye molecules are prone to leak through the liquid-liquid interface. As a result, measured signal is averaged between droplets and the reliability of the assay is decreased.²⁹⁻³⁴ It has been proposed that the dye “leakage” into neighboring droplets is facilitated by micellar³² or vesicular structures³⁴ which act as carriers between droplets. The exchange between droplets has also been demonstrated with fluorescein³⁵ and methylumbelliferone dyes.³⁶

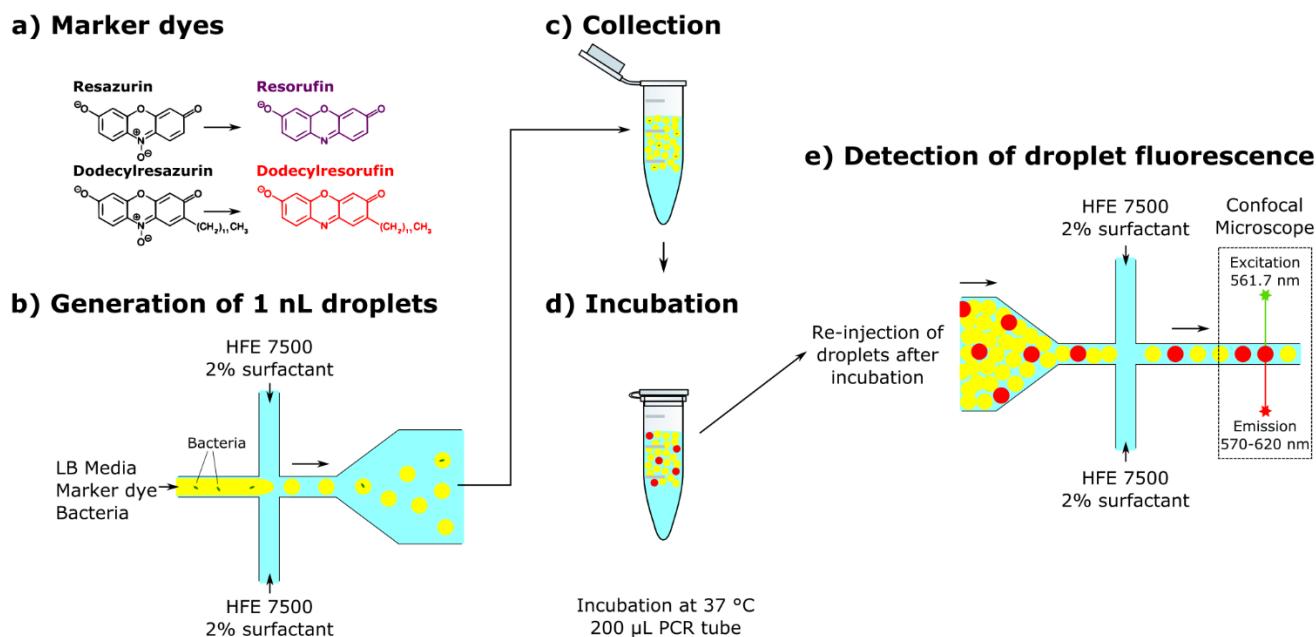


Figure 1. Marker dyes and schematic of a microfluidic experiment. a) Metabolic marker dyes resorufin and dodecylresorufin (C12R), and their respective substrates. Note: colors of resorufin (purple) and C12R (red) do not reflect their actual color and fluorescence (which are similar). b) Encapsulation of bacteria (*E.coli* or *E.aerogenes*), growth medium LB and dye substrate (resazurin or dodecylresazurin) into 1nL droplets using flow-focusing junction in PDMS chip. c) Collection of droplet emulsion into 200 μL PCR tube. d) Incubation of droplets at 37 °C. e) Detection of droplet fluorescence in second PDMS chip that was mounted on confocal microscope stage. Droplets were injected to the chip and separated by additional stream of oil in flow-focusing junction. Resorufin/C12R fluorescence of each droplet was measured using confocal microscope (Ex 561.7 nm/Em 570-620 nm).

A number of approaches have been used to tackle the problem of resorufin leakage between droplets. For instance, using FC-40 fluorocarbon, instead of the most common HFE-7500 liquid, increases the retention of resorufin in droplets, but at the expense of the emulsion quality and stability.²⁹ Decreasing the concentration of surfactant^{32,34} and addition of BSA³² or sugar additives to the aqueous phase³⁰ has been shown to decrease the leakage of resorufin. A new class of nanoparticle (NP) surfactants has also been demonstrated to efficiently increase the maintenance of resorufin in droplets. This is a very promising solution, still to be fully validated against potential interaction of some proteins with the surface of NPs.³³

Here we propose an alternative path to reduce the dye leakage by using modified viability marker compound instead of traditional resorufin. We recommend the use of dodecylresorufin (C12R), a derivative of resorufin with similar fluorescent properties, as a viability marker in droplet microbial assays. It has been suggested previously that C12R is maintained for longer periods of time in aqueous droplets. So far no thorough research, especially with live organisms in viability assay, has been carried out.³¹ Herein, we thoroughly evaluated the performance of resorufin and C12R in bacterial assays in emulsions comprising of thousands of nanoliter monodisperse droplets.

RESULTS AND DISCUSSION

In our experiments we compared the performance of two different metabolic marker dyes: resorufin and C12R (Fig. 1a).

In order to differentiate their performance we ran a number of droplet microfluidic assays with different bacteria. We used the two marker dyes to distinguish between positive (bacteria containing) and negative (empty) droplets. The substrates of both dyes, resazurin and dodecylresazurin respectively, get converted to highly fluorescent products by the aerobic metabolism of organisms. We used the 50 μM concentration of the dye substrates in our experiments to, a value similar to those used in previous applications of resazurin in droplet microfluidic systems.^{7,8,37}

We tested the marker dyes with two different bacteria. First, with commonly used test bacteria *E.coli* that contained enhanced Green Fluorescent Protein (eGFP) coding plasmid for additional signal control. The eGFP signal served as a reference for the droplets containing bacteria. Second, we tested the dyes with *E.aerogenes* that has over the last decades been increasingly associated with nosocomial infections.³⁸

In our experiments we encapsulated bacteria into 1nL droplets (exact size distribution shown in SI Figure S2) with respective dye substrates using flow-focusing junction on a polydimethylsiloxane (PDMS) chip (Fig 1b) that was described in detail by Kaminski *et al.*³⁹ We adjusted the concentration of bacteria in the droplet phase so that ~20 % of generated droplets contained bacteria. According to Poisson distribution² ~18% of droplets contain single colony forming unit (CFU) of bacteria while ~2% has more than one CFU in these conditions.

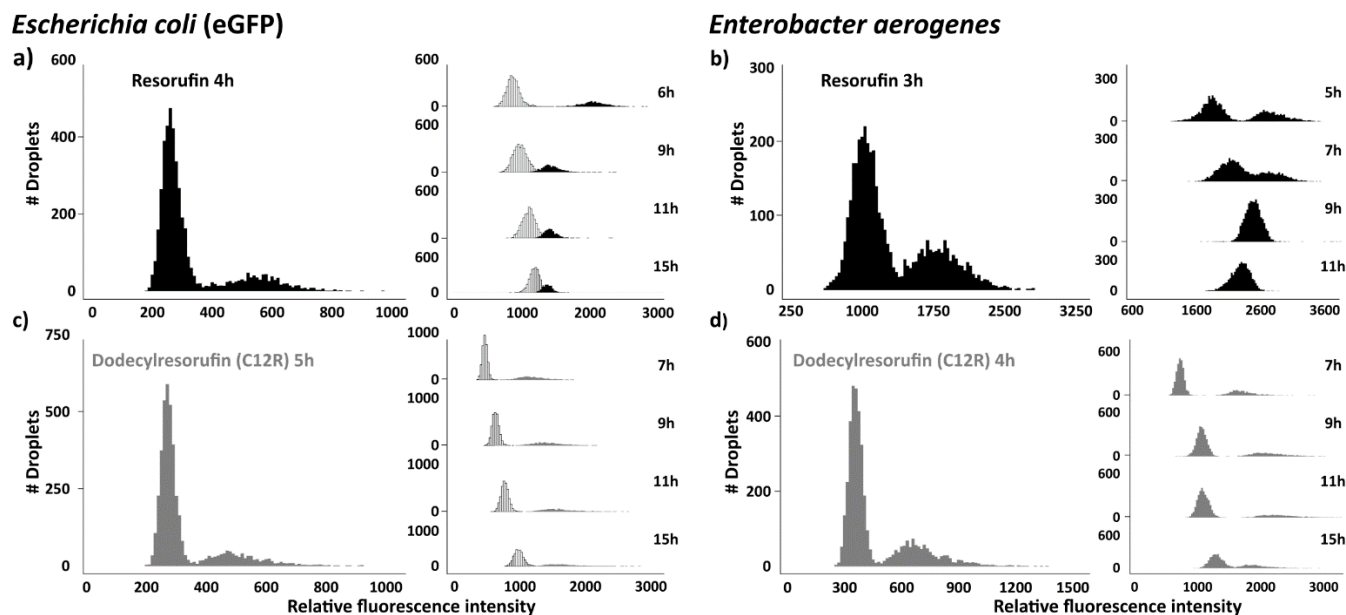


Figure 2. Histograms depicting distribution of droplet fluorescence after different incubation times. X-axes show the relative fluorescence of droplet and Y-axes show number of droplets with that particular intensity. Droplet intensities obtained with resorufin marker dye are shown for *E.coli* (a) and *E.aerogenes* (b), similarly C12R results are shown for the same bacteria (cd). Bigger left panel shows the bimodal histogram of the results from particular incubation time when the positive bacteria-containing droplets (right peak) were first clearly distinguishable from empty droplets (left peak). On the right panel similar results are given for the longer incubation times. Please note that histograms of empty droplets are shown with white background for *E.coli* (according to lack of eGFP signals in droplets).

We used the HFE 7500 fluorocarbon liquid as the continuous phase. This oil ensures good stability of emulsion over time.²⁹ Although previous report has shown that the decrease of surfactant concentration reduces resorufin leakage³², we used relatively high 2% concentration of PFPE-PEG-PFPE triblock surfactant concentration to provide for good stability of the emulsions against coalescence during long-term incubation.

After generation we collected droplets into 200 μ L PCR tubes (Fig. 1c) for off-chip incubation at 37 °C (Fig. 1d). After incubation we injected the droplets into a separate chip for analysis (Fig. 1e). This second chip contained flow-focusing junction to provide the additional spacing between the droplets prior the measurement.

We used a confocal microscope to measure the intensity of fluorescence emitted from droplets. The time between the generation of a droplet library and the measurement ranged from three hours (four with *E.coli*) to 24 hours in the longest experiments. To understand which droplets contain bacteria, we first executed the assays on *E.coli* expressing eGFP. The droplets with increased eGFP signals were distinguishable from background droplets after six hours of incubation. Thus, we chose the eGFP signal to mark the droplets containing *E.coli* bacteria at incubation time-points from 6 to 24 hours.

Intensity and stability of the signal from the dyes.

We found that negative droplets (i.e. ones without bacteria) containing resorufin exhibit higher baseline fluorescence than the negative droplets containing C12R. We had to use higher laser power and to set higher sensitivity to the microscope detector during interrogation of droplets containing C12R in order to obtain comparable fluorescence intensities (see Figures S5-S8 for exact details of confocal microscope settings).

The increase of fluorescence intensity from resorufin in 1 nL droplets was faster than the increase of fluorescence from C12R, both with *E.coli* and with *E.aerogenes*. We could distinguish the positive droplets from the background (negative droplets) in assays based on resorufin already after four and three hours, respectively for *E.coli* and *E.aerogenes* (Fig. 2ab, left panels). With C12R the time to distinguish positive droplets was five hours for *E.coli* and four hours for *E.aerogenes* (Fig. 2cd, left panels). It is difficult to speculate on the reason behind that difference in fluorescent signal increase as the mechanism of converting rezasurin to fluorescent product is not fully understood and it is not even sure if it occurs in the cell or outside in the medium.²³ There can be several explanations. Firstly, long hydrocarbon tail may simply slow down the intake of the substrate in case of dodecylresazurin if the process occurs in the cells. Secondly, the hydrocarbon tail may disturb the interaction with reducing enzymes. Thirdly, the fluorescent properties of dye molecules can be behind the difference. Fluorescence of resorufin is stronger and it is thus easier to distinguish from background. We would exclude the effect of C12R of general metabolism of bacteria. In our case, we did not observe any significant difference in bacterial growth with different dye molecules, as demonstrated by similar GFP signal increase in droplets over time (Figure S3).

Although the use of C12R requires slightly longer incubation to distinguish the positive droplet than resorufin, it provides for a more stable signal over time. In our experiments we could distinguish positive droplets from empty droplets over a longer period of time with C12R in case of both *E.coli* and *E.aerogenes* (Fig. 2). The fluorescence of resorufin in positive droplets quickly starts diminishing as the dye leaks to empty droplets and the overall signal is averaged. The leakage is faster in the case of assays with *E.aerogenes* where positive

and negative droplet signals are indistinguishable already after nine hours (Fig. 2 ab, right panels). Using C12R we were able to distinguish the populations of positive and negative droplets

clearly after 15 hours with both bacteria (Fig. 2cd, right panels).

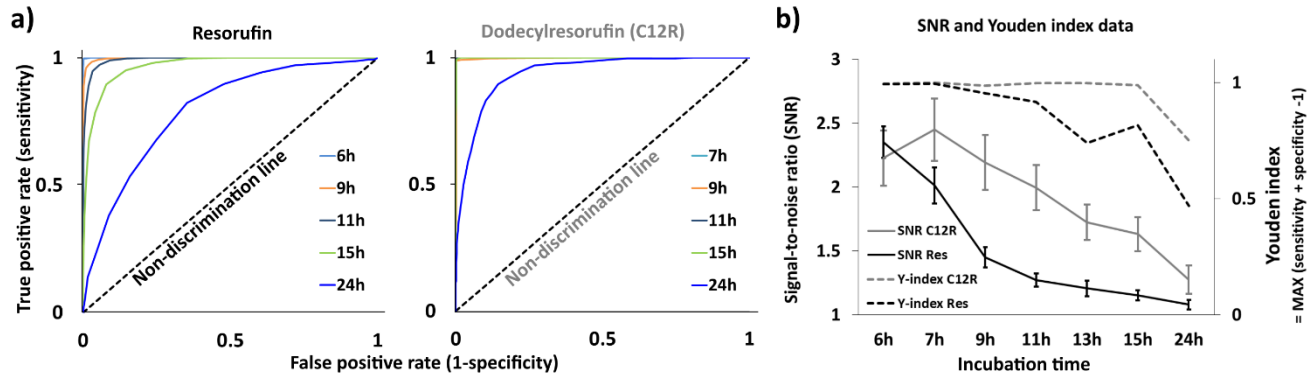


Figure 3. a) Receiver Operating Characteristic (ROC) curves with resorufin and C12R after different incubation times ranging from 6 to 24h. X-axis shows False positive and Y-axis True positive rates. Curves close to upper left corner (0, 1) are accurate, while getting closer to diagonal “No-discrimination line” shows inaccuracy. b) Youden index and signal-to-noise ratio (SNR) data for both marker dyes after different incubation times. Youden index shows the combined value of sensitivity and specificity (it is presented as dotted lines on secondary axis). SNR values are shown on primary axis as median fluorescence intensity ratios of positive droplets to empty droplets. Error bars show +/- 1 median absolute deviation (MAD).

Accuracy of the assay - the true-positive and true-negative rates.

Throughout this article we use the term “accuracy” to indicate the combined values of sensitivity and specificity, similarly to the way this term is used in the previous report on droplet-based assays.⁴⁰ Sensitivity is defined as the true positive rate (the fraction of all the positive droplets that is correctly identified as positive in the assay). In turn, specificity is the true negative rate (i.e. the fraction of all the negative droplets that is correctly identified as negative). For example, we start with an assay comprising 100 droplets in total, with 10 of them containing bacteria. At the end of the assay, say we measured 12 droplets being positive (8 of them correctly plus 4 false positives). 2 truly positive droplets were identified as being negative (false negatives). In that scenario, the sensitivity of this assay is $(10-2)/10=80\%$ and the specificity is $(90-4)/90\approx 96\%$.

In leaky droplet assays the sensitivity and specificity decrease over time because the marker dye diffuses from positive droplets to neighboring negative droplets.⁴⁰ Thus, truly positive droplets present lower fluorescence and can be incorrectly counted as negative drops (a false negative), and vice versa the negative drops acquire the fluorescently active molecules that can cause a false positive readout.

We used Receiver Operating Characteristic (ROC) curves to analyze how accurately the two marker dyes distinguish the positive and negative droplets. The ROC curve is a common statistical tool used to visualize the accuracy of a diagnostic test. The curves are created by plotting the True Positive (sensitivity) and the False Positive (1-specificity) rates at different threshold levels. With accurate assays the ROC curve nears the upper left corner (0,1), while in inaccurate assay the curve lays down towards the diagonal “Non-discrimination” line.⁴⁰⁻⁴² Fig. 3a compares the ROC curves of resorufin and C12R at different *E.coli* incubation times. C12R provides for better accuracy over time as the curves remain in the upper left (0, 1) corner during most of the the experiment. With resorufin the

curves rapidly start moving towards the “no-discrimination” line indicating the quick loss of accuracy over time.

C12R provides for better Youden index scores.

In order to analyze ROC curves more thoroughly, we calculated the Youden index (J) that shows the combined value of sensitivity and specificity ($J = \text{sensitivity} + \text{specificity} - 1$). The Youden index is a dimensionless number acquiring values between 0 and 1. An assay having perfect sensitivity and specificity results in $J=1$, while when the ROC curve approaches the diagonal no-discrimination line $J=0$.^{40,41,43,44} In general, large J values indicate accurate droplet-based assays.⁴⁰

We show the values of the Youden index for both marker dyes at different time points in Fig. 3b. C12R has better accuracy than resorufin as the J value remains close to 1 for most of the experiment and begins to drop significantly only at the 24h checkpoint. In the case of resorufin the decrease commences already after seven hours.

C12R assays exhibit increased signal to noise ratio.

Another key parameter in any droplet-based assay is the signal-to-noise ratio (SNR). SNR indicates the difference between the fluorescence intensity of bacteria containing (positive) and empty (negative) droplets. In order to establish the SNR values for experiments with resorufin and C12R we measured the respective droplet fluorescence intensities for positive and negative droplets and calculated the median values for both. The graph in Fig. 3b shows the SNR values for resorufin and C12R as black and grey line on the primary axis, respectively. This data demonstrates that the C12R has higher SNR than resorufin for most of the incubation time, except after six hours of incubation when they were relatively equal within the margin of error.

Accuracy and SNR versus concentration of bacteria

Next, we tested the accuracy of both resorufin and C12R at different concentrations of bacteria. We compared the results of the experiment described above (~20% droplets with *E.coli*)

with results on droplet emulsions containing ~10 and 32 % of positive droplets. Fig. 4a shows the values of the Youden index for both dyes at different concentrations of bacteria. Accuracy with C12R (grey lines) surpasses the resorufin results (black lines) at all bacteria concentrations. The C12R demonstrates high accuracy at all concentrations for 15 hours as the J value remains close to 1. In contrast, for resorufin, the J value starts to decrease already after seven hours of incubation with all bacteria concentrations.

When we looked deeper into the Youden index data (Figure S11) we noticed that with both dyes the decrease in specificity tends to be greater compared to the drop in sensitivity over time. This demonstrates again that the dye leakage from positive droplets (which is more intense with resorufin) increases the fluorescence of empty droplets which in turn increases the probability of scoring a false positive result.

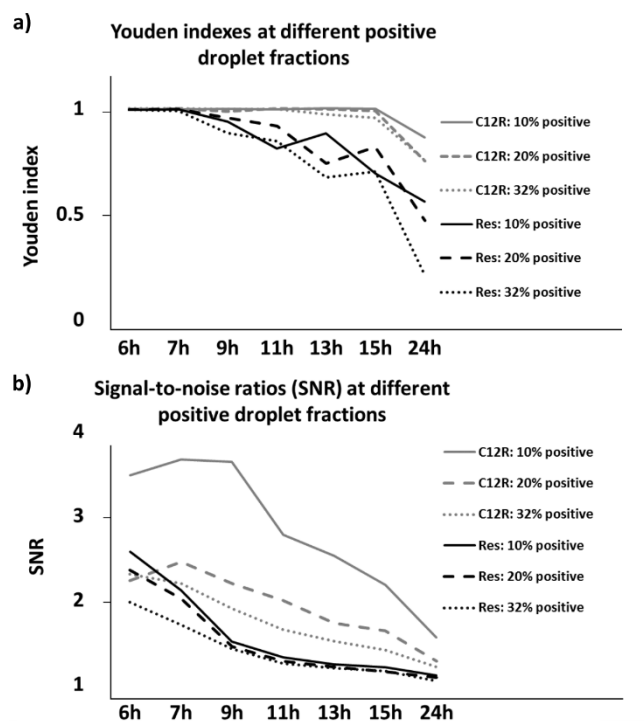


Figure 4. Youden index and signal-to-noise ratio (SNR) graphs after different incubation times. Resorufin (black) and C12R (grey) viability dyes were tested with different positive (bacteria containing) droplet concentrations (10, 20 and 32%). a) Graph showing the Youden index of dyes after different incubation times. b) SNR data after different incubation times for both dyes.

We also compared the SNR of both dyes at different bacteria concentrations. The graph on Fig. 4b depicts SNR ratios measured for resorufin (black lines) and C12R (grey lines) with various bacteria concentrations after different incubation times. In our experiments C12R constantly outperformed the resorufin in terms of SNR level. For all three different bacteria concentrations tested after various incubation times the C12R showed higher SNR values compared with resorufin. Only exception, when the SNR values were similar, was after six hours of incubation in 20% positive droplet experiment.

The rate of leakage of the dye versus the concentration of bacteria.

With both dyes we observed higher noise (manifested by lower values of SNR) in libraries containing a higher fraction of positive droplets (Fig. 4b). For a rough estimation we can safely assume that during incubation the droplets are densely packed in tube according to the Kepler conjecture. In such assembly, each droplet is in contact with 12 neighboring droplets in three-dimensional space.⁴⁵ We ran experiments with 10, 20 and 32% of droplets containing bacteria. With Kepler conjecture assumption it means that each empty droplet had roughly ~1.2, ~2.4 and ~3.8 neighbors that contained bacteria, respectively. Combining this fact with our SNR data from different positive droplet fractions (Fig. 4b) we have demonstrated that the leakage of resorufin/C12R to empty droplets depends on the number of neighboring positive droplets. This experimental observation is in good agreement with leaky droplet-based assay theoretical study that was described by Chen and colleagues who modelled the signal leakage between droplets in two-dimensional space where each droplet has 6 neighbors. Their model also showed that the leakage into negative droplets is related to the number of positive neighbours.⁴⁰

Latest research shows that the surfactant assisted formation of vesicular structures³⁴ can be the mechanism for the transport of small molecules like fluorophores between droplets. The “less-leaky” behavior of the C12R can then be associated with the decreased ability to partitioning into these structures due to the presence of extra 12-carbon long chain in the dye molecule (Fig. 1). There can be many explanations (or combinations of them) for such disfavored partitioning. Firstly, the fluorinated core of such vesicles may hinder the packaging of molecules with long lipophilic side-chains. Secondly, the C12 chain may reduce the number of fluorophores inside vesicles due to the larger size. Thirdly, the size of the vesicle can be bigger, resulting in slower transport of fluorophores between droplets. Thorough analysis of such potential mechanisms would require development of “minimal emulsion” system as described by Gruner *et al.* as such effects are difficult to analyze in bulk emulsions.³⁴ Proper analysis of the effect would also benefit from availability of resorufin molecules with hydrocarbon side chains of different length. Thorough analysis of the mechanisms behind the better retention of molecules with hydrocarbon side-chains would be highly useful from the droplet assay perspective. We believe that our research here is only a first step towards understanding the reasons behind that phenomenon.

CONCLUSIONS

World Health Organization has set up a Global Action plan to tackle the antimicrobial resistance. One part of Objective Five of that plan calls for the development of new diagnostic tools for that purpose.⁴⁶ Droplet-based detection and analysis of bacteria is one of the most promising technologies suitable for such rapid diagnostics as demonstrated by recent research.^{3,5} With our experiments we present an easily adaptable solution to the long known intensive dye leakage problem in droplet microfluidics associated with heavily used viability marker dye resorufin.^{30,32,34,40}

We compared the performance of resorufin and C12R as markers of bacterial metabolism in micro-droplet assays. We analyzed and compared five main parameters: fluorescence intensity, detection time of positive droplets, duration of time when positive and negative droplets are distinguishable, sig-

nal-to-noise ratio (SNR) and accuracy of marker dyes (sensitivity + specificity) in distinguishing bacteria containing droplets presented as ROC curves and Youden index. Table 1 summarizes and compares the performance of the two marker dyes. Resorufin has stronger fluorescence and provides for slightly faster detection. The C12R is more useful in terms of longer cultivation time and it also clearly outperforms resorufin in terms of the accuracy and signal to noise ratio over time.

	Resorufin	Dodecylresorufin
General fluorescence intensity	+	-
Detection time	+	-
Positive droplet differentiation duration	-	+
Sensitivity + Specificity (ROC, Youden index)	-	+
Signal-to-noise ratio (SNR)	-	+

Table 1. Comparison between resorufin and C12R in droplet microfluidic bacterial assay.

Based on our experiments we conclude that C12R presents significant advantages over resorufin in droplet assays, especially with regard to the consistently higher accuracy rating. It is of utmost importance in any diagnostics assay to have as high accuracy as possible to maximize correct calls while minimizing the erroneous ones.^{41,47,48} Also the ability of C12R to differentiate bacteria containing droplets over longer periods of time opens up possibilities to design assays with broader detection time-window or tests with multiple detection time-points.

The method that we described here is only one of many possible ways to tackle the problem of resorufin leakage between droplets. A number of studies attempted to address leakage issue, either by using specific oil type,²⁹ lowering surfactant concentration^{32,34} or by using special additives in droplets.^{30,32,35} It has been also advocated that new surfactants and dye molecules should be synthesized to bypass the challenge to derive a droplet-tight dye. For example introducing novel coumarin dyes with hydrophilic sulfonate groups that prevent dye leakage.¹⁴

Still, the synthesis of new compounds can be difficult and time consuming, and cannot be performed easily in laboratories lacking synthetic chemistry capability.⁴⁰ The most interesting and also the most promising approach so far, has been the use of nanoparticles for the stabilization of droplets and prevention of fluorophore leakage.³³ Recently this method has been supplemented with coating of the nanoparticles with bovine serum albumin to increase the compatibility of the interface with enzymes.³⁷ While all of these technologies reduce the leakage of resorufin from droplets, we propose on the basis of the analysis presented here that it may be efficient and facile strategy to simply replace resorufin with less leaky fluorophores like C12R. This approach is immediately available without the need for additional testing regarding biocompatibility or droplet formation and stability. Dodecylresazurin can be directly used in all assays previously described with conventional resazurin.

It also seems to be a viable idea to combine the choice of the dye with the other strategies increasing the retention of dye in droplets. Especially, the combination of C12R assays with addition of BSA³² or nanoparticle-based stabilizers^{33,37} could result in fluorescent signal retention in droplets with unprecedented stability and duration as these technologies individually still exhibit some leakage over time.

Here we demonstrated that C12R is compatible with Gram negative bacteria *E.coli* and *E.aerogenes* in droplet-based assays. One of the remaining key challenges is to verify the compatibility of C12R with a larger number of various microorganisms. Due to the high similarity we expect C12R to be equally usable as resorufin that has also been used for droplet-based analysis of Gram positive bacteria *Staphylococcus aureus*.¹ Theoretically C12R can be used with all aerobic microorganisms as the conversion of substrate resazurin to highly fluorescent resorufin has been demonstrated to be related to aerobic metabolism in microorganisms.¹⁹

The potential applications of the C12R dye in droplet assays definitely include droplet digital quantification of bacteria that so far has only been demonstrated with resorufin as enzymatic activity marker.² With the latest advances in improving the design of digital assays, the number of partitions/droplets required for high precision and dynamic range has been greatly diminished.⁴⁹ That minimizes the technical requirements needed for running digital assays and increases its' potential availability to multiple new formats, including digital counting of bacteria. We also foresee that the analysis of antibiotic susceptibility could benefit from our findings as resorufin-based assays have been shown, but only in physically separated droplets stored sparsely in long channels to prevent transfer of the dye between droplets.^{1,7} Being able to use thousands of droplets in densely packed emulsions will enable transforming the assays to medium- and high-throughput format. In a wider view, we hope that the longer fluorescence retention of C12R in droplet opens up new possibilities in high-throughput screening and research in microbiology. Especially when combined with recent developments in microfluidic techniques that allow droplet sorting¹⁶ and parallelized ultra-high-throughput generation⁵⁰ and interrogation of droplets.⁵¹

MATERIALS AND METHODS

Microfluidics

In our experiments we used two different microfluidic chips. One for generation of droplets and second one for droplet analysis. Both chips were made of a polydimethylsiloxane (PDMS) fluidic layer that was plasma bonded to 1mm-thick glass slide. See Figure S1 for details. Fabrication of fluidic layer was as follows: in the first step we fabricated the polycarbonate moulds in 5 mm plates of polycarbonate (MacrocLEAR, Bayer, Germany) using a CNC milling machine (MSG4025, Ergwind, Poland). Next, we poured PDMS (Sylgard 184, Dow Corning, USA) onto the PC chip and subsequently polymerized the mold at 95 °C for 45min. In a following step, we silanized the PDMS mold for 3h under 10 mbar pressure with vapors of tridecafluoro-1,1,2,2,-tetrahydrooctyl)-1-trichlorosilane (Alfa Aesar, Germany). Cleaned PDMS negative masters served for molding of the positive PDMS replicas that we subsequently bonded with glass slide by exposing both parts to 30s oxygen plasma and placing them together.

We modified the microfluidic channels hydrophobically by filling the chip with Novec 1720 (3M, United States) for 10 minutes. After fluid evaporation at room temperature the chips were baked at 135 °C for 1h to preserve modification. We controlled the flow of oil and reagents in microfluidic experiments with neMESYS syringe pumps (Cetoni, Germany). Droplets were generated with ~300 Hz frequency and collect-

ed for off-chip incubation in 16 separate 200 μ L tubes with each different experiment.

Bacteria

We used two different bacteria in our experiments: *Escherichia coli* DH5 α placEGFP (a kind gift from Prof. Douglas Weibel, Department of Biochemistry, University of Wisconsin-Madison) and *Enterobacter aerogenes* PCM183 (Polish Collection of Microorganisms). For bulk culture of bacteria and cultivation in droplets we used LB-Lennox media (Roth, Germany). With *E. coli* the media contained 100 μ g/mL ampicillin and 1mM isopropyl β -D-1-thiogalactopyranoside (both from Thermo Fischer Scientific, USA) for eGFP plasmid retention and expression. We diluted overnight cultures of bacteria ~100X into fresh media and incubated until the bacteria entered exponential growth phase. Next, we diluted the bacteria suspension in media for droplet generation. Bulk concentration of bacteria was estimated using DEN-1 densitometer (Biosan SIA, Latvia).

Reagents

We used NovecTM HFE 7500 fluorocarbon oil (3M, USA) with 2% PFPE-PEG-PFPE surfactant (synthesized according to protocol published by Holtze *et al.*⁵²). Dye substrates resazurin sodium salt (Sigma Aldrich, Germany) or C12-resazurin (part of Vybrant[®] Cell Metabolic Assay Kit, Life Technologies, USA) were used as 50 μ M solution in LB in all assays. Final media solution contained 1% dimethylsulfoxide (Life Technologies, USA) that was used for solubilization of dye. We used the pipette tip shaking to mix concentrated dye solutions with media in test-tube as heavy vortexing caused C12R to attach onto tube walls. Tracer dye Rhodamine 110 (Sigma-Aldrich, Germany) was dissolved in aqueous phase at 0.1 μ M concentration. Final dye solutions in media were filtered using Chromafil[®] Xtra PET 45/25 filters (Macherey-Nagel, Germany) to remove unsolved dye particles.

Fluorescence measurement and data analysis

We measured the fluorescence of droplets using droplet reading chip that was mounted onto the stage of A1R confocal microscope (Nikon, Japan). We acquired fluorescence of eGFP and Rhodamine 110 at excitation/detection wavelengths at 488nm/500-550nm and in the case of resorufin/C12R at 516.7nm/570-620nm, respectively. We took the fluorescent readouts of droplets after 0h, 3h (*E. aerogenes* only), 4h, 5h, 6h, 7h, 9h, 11h, 13h, 15h and 24h incubation. We used different sample aliquots from droplet collection at each time-point. We analyzed ~4000 droplets at each incubation time-point at a ~600 Hz frequency. We analyzed the raw fluorescence data using MS Office Excel (Microsoft, USA) with Real Statistics Resource Pack (<http://www.real-statistics.com/>). Droplet signals stand for peak relative fluorescence intensities allocated to each droplet. We also calculated ROC curves and Youden indexes⁴⁰⁻⁴² for measuring the performance of the dyes (see Note S1 for detailed information).

ASSOCIATED CONTENT

Supporting information

The Supporting Information is available free of charge on the ACS Publications website.

Microfluidic chip schematics, droplet size analysis, ROC and Youden explanation and data, droplet fluorescence histograms at different incubation time-points (PDF)

AUTHOR INFORMATION

Corresponding Author

* garst@ichf.edu.pl

Author Contributions

OS, TSK and PG conceived the idea of the study. OS and TSK designed the experiments. OS and AR executed the experiments. OS analyzed the data and was responsible for writing the manuscript.

The manuscript was written through contributions of all authors. / All authors have given approval to the final version of the manuscript.

ACKNOWLEDGEMENTS

Project co-financed by the European Research Council Starting Grant 279647 and National Science Centre funding based on decision number: DEC-2014/12/W/NZ6/00454 (Symfonia). This work was also supported by the Estonian Research Council grant PUTJD589 (to O.S.), Foundation for Polish Science MISTRZ fellowship (to P.G.) and grant VENTURES/2012-10/4 (to T.S.K.). T.S.K. obtained the funds for the preparation of the doctoral dissertation from the National Centre for Science within the scholarship on the basis of the decision number DEC-2014/12/T/ST4/00649. This project was partially performed in the laboratories founded by Nano-Fun POIG.02.02.00-00-025/09.

REFERENCES

- Boedicker, J. Q.; Li, L.; Kline, T. R.; Ismagilov, R. F. Detecting Bacteria and Determining Their Susceptibility to Antibiotics by Stochastic Confinement in Nanoliter Droplets Using Plug-Based Microfluidics. *Lab Chip* **2008**, *8*, 1265–1272.
- Najah, M.; Griffiths, A. D.; Ryckelynck, M. Teaching Single-Cell Digital Analysis Using Droplet-Based Microfluidics. *Anal. Chem.* **2012**, *84* (3), 1202–1209.
- Kang, D.-K.; Gong, X.; Cho, S.; Kim, J.-Y.; Edel, J. B.; Chang, S.-I.; Choo, J.; DeMello, A. J. 3D Droplet Microfluidic Systems for High-Throughput Biological Experimentation. *Anal. Chem.* **2015**, *87*, 10770–10778.
- Lyu, F.; Xu, M.; Cheng, Y.; Xie, J.; Rao, J.; Tang, S. K. Y. Quantitative Detection of Cells Expressing BlaC Using Droplet-Based Microfluidics for Use in the Diagnosis of Tuberculosis. *Biomicrofluidics* **2015**, *9* (4), 044120.
- Kang, D.-K.; Ali, M. M.; Zhang, K.; Huang, S. S.; Peterson, E.; Digman, M. A.; Gratton, E.; Zhao, W. Rapid Detection of Single Bacteria in Unprocessed Blood Using Integrated Comprehensive Droplet Digital Detection. *Nat. Commun.* **2014**, *5* (5427).
- Eun, Y.; Utada, A. S.; Copeland, M. F.; Takeuchi, S.; Weibel, D. B. Encapsulating Bacteria in Agarose Microparticles Using Microfluidics for High-Throughput Cell Analysis and Isolation. *ACS Chem. Biol.* **2011**, *6*, 260–266.
- Churski, K.; Kaminski, T. S.; Jakiela, S.; Kamysz, W.; Baranska-Rybak, W.; Weibel, D. B.; Garstecki, P. Rapid Screening of Antibiotic Toxicity in an Automated Microdroplet System. *Lab Chip* **2012**, *12*, 1629–1637.
- Boitard, L.; Cottinet, D.; Bremond, N.; Baudry, J.; Bibette, J. Growing Microbes in Millifluidic Droplets. *Eng. Life Sci.* **2015**, *15* (3), 318–326.
- Baraban, L.; Bertholle, F.; Salverda, M. L. M.; Bremond, N.; Panizza, P.; Baudry, J.; de Visser, J. A. G. M.; Bibette, J. Millifluidic Droplet Analyser for Microbiology. *Lab Chip* **2011**, *11*, 4057–4062.
- Jakiela, S.; Kaminski, T. S.; Cybulski, O.; Weibel, D. B.; Garstecki, P. Bacterial Growth and Adaptation in Microdroplet Chemostats. *Angew. Chem. Int. Ed. Engl.* **2013**, *52* (34), 8908–8911.
- Jarosz, D. F.; Brown, J. C.; Walker, G. A.; Datta, M. S.; Ung, W. L.; Lancaster, A. K.; Rotem, A.; Chang, A.; Newby, G. A.; Weitz, D. A.; Bisson, L. F.; Lindquist, S. Cross-Kingdom



- Chemical Communication Drives a Heritable, Mutually Beneficial Prion-Based Transformation of Metabolism. *Cell* **2014**, *158* (5), 1083–1093.
- (12) Park, J.; Kerner, A.; Burns, M. A.; Lin, X. N. Microdroplet-Enabled Highly Parallel Co-Cultivation of Microbial Communities. *PLoS One* **2011**, *6* (2), e17019.
- (13) Weitz, M.; Mückl, A.; Kapsner, K.; Berg, R.; Meyer, A.; Simmel, F. C. Communication and Computation by Bacteria Compartmentalized within Microemulsion Droplets. *J. Am. Chem. Soc.* **2014**, *136*, 72–75.
- (14) Najah, M.; Mayot, E.; Mahendra-Wijaya, I. P.; Griffiths, A. D.; Ladame, S.; Drevelle, A. New Glycosidase Substrates for Droplet-Based Micro Fluidic Screening. *Anal. Chem.* **2013**, *85* (20), 9807–9814.
- (15) Scanlon, T. C.; Dostal, S. M.; Griswold, K. E. A High-Throughput Screen for Antibiotic Drug Discovery. *Biotechnol. Bioeng.* **2014**, *111* (2), 232–243.
- (16) Baret, J.-C.; Müller, O. J.; Taly, V.; Ryckelynck, M.; El-Harrak, A.; Frenz, L.; Rick, C.; Samuels, M. L.; Hutchison, J. B.; Agresti, J. J.; Link, D. R.; Weitz, D. A.; Griffiths, A. D. Fluorescence-Activated Droplet Sorting (FADS): Efficient Microfluidic Cell Sorting Based on Enzymatic Activity. *Lab Chip* **2009**, *9*, 1850–1858.
- (17) Lim, S. W.; Tran, T. M.; Abate, A. R. PCR-Activated Cell Sorting for Cultivation-Free Enrichment and Sequencing of Rare Microbes. *PLoS One* **2015**, *10* (1), e0113549.
- (18) Guerin, T. F.; Mondido, M.; McClenn, B.; Peasley, B. Application of Resazurin for Estimating Abundance of Contaminant Degrading Micro Organisms. *Letts. Appl. Microbiol.* **2001**, *32*, 340–345.
- (19) Karakashev, D.; Galabova, D.; Simeonov, I. A Simple and Rapid Test for Differentiation of Aerobic from Anaerobic Bacteria. *World J. Microbiol. Biotechnol.* **2003**, *19*, 233–238.
- (20) Mariscal, A.; Lopez-Gigosos, R. M.; Carnero-Varo, M.; Fernandez-Crehuet, J. Fluorescent Assay Based on Resazurin for Detection of Activity of Disinfectants against Bacterial Biofilm. *Appl. Microbiol. Biotechnol.* **2009**, *82*, 773–783.
- (21) Martín-Navarro, C. M.; López-Arencibia, A.; Sifaoui, I.; Reyes-Battle, M.; Cabello-Vílchez, A. M.; Maciver, S.; Valladares, B.; Piñero, J. E.; Lorenzo-Morales, J. PrestoBlue® and AlamarBlue® Are Equally Useful as Agents to Determine the Viability of *Acanthamoeba* Trophozoites. *Exp. Parasitol.* **2014**, *145*, S69–S72.
- (22) Sarker, S. D.; Nahar, L.; Kumarasamy, Y. Microtitre Plate-Based Antibacterial Assay Incorporating Resazurin as an Indicator of Cell Growth, and Its Application in the In Vitro Antibacterial Screening of Phytochemicals. *Methods* **2007**, *42* (4), 321–324.
- (23) O'Brian, J.; Wilson, I.; Orton, T.; Pognan, F. Investigation of the Alamar Blue(resazurin) Fluorescent Dye for the Assessment of Mammalian Cell Cytotoxicity. *Eur. J. Biochem.* **2000**, *267*, 5421–5426.
- (24) Liu, Y.; Jung, S. Y.; Collier, C. P. Shear-Driven Redistribution of Surfactant Affects Enzyme Activity in Well-Mixed Femtoliter Droplets. *Anal. Chem.* **2009**, *81*, 4922–4928.
- (25) Bui, M.-P. N.; Li, C. A.; Han, K. N.; Choo, J.; Lee, E. K.; Seong, G. H. Enzyme Kinetic Measurements Using a Droplet-Based Microfluidic System with a Concentration Gradient. *Anal. Chem.* **2011**, *83*, 1603–1608.
- (26) Hess, D.; Rane, A.; DeMello, A. J.; Stavrakis, S. High-Throughput, Quantitative Enzyme Kinetic Analysis in Microdroplets Using Stroboscopic Epifluorescence Imaging. *Anal. Chem.* **2015**, *87*, 4965–4972.
- (27) Abalde-Cela, S.; Gould, A.; Liu, X.; Kazamia, E.; Smith, A. G.; Abell, C. High-Throughput Detection of Ethanol-Producing Cyanobacteria in a Microdroplet Platform. *Interface* **2015**, *12* (106).
- (28) Wang, B. L.; Ghaderi, A.; Zhou, H.; Agresti, J. J.; Weitz, D. A.; Fink, G. R.; Stephanopoulos, G. Microfluidic High-Throughput Culturing of Single Cells for Selection Based on Extracellular Metabolite Production or Consumption. *Nat. Biotechnol.* **2014**, *32* (5), 473–478.
- (29) Mazutis, L.; Baret, J.-C.; Treacy, P.; Skhiri, Y.; Araghi, A. F.; Ryckelynck, M.; Taly, V.; Griffiths, A. D. Multi-Step Microfluidic Droplet Processing: Kinetic Analysis of an In Vitro Translated Enzyme. *Lab Chip* **2009**, *9*, 2902–2908.
- (30) Sandoz, P. A.; Chung, A. J.; Weaver, W. M.; Carlo, D. Di. Sugar Additives Improve Signal Fidelity for Implementing Two-Phase Resorufin-Based Enzyme Immunoassays. *Langmuir* **2014**, *30*, 6637–6643.
- (31) Stapleton, J. A.; Swartz, J. R. Development of an In Vitro Compartmentalization Screen for High-Throughput Directed Evolution of [FeFe] Hydrogenases. *PLoS One* **2010**, *5* (12), e15275.
- (32) Skhiri, Y.; Gruner, P.; Semin, B.; Brosseau, Q.; Pekin, D.; Mazutis, L.; Goust, V.; Kleinschmidt, F.; El Harrak, A.; Hutchison, J. B.; Mayot, E.; Bartolo, J.-F.; Griffiths, A. D.; Taly, V.; Baret, J.-C. Dynamics of Molecular Transport by Surfactants in Emulsions. *Soft Matter* **2012**, *8* (41), 10618–10627.
- (33) Pan, M.; Rosenfeld, L.; Kim, M.; Xu, M.; Lin, E.; Derda, R.; Tang, S. K. Y. Fluorinated Pickering Emulsions Impede Interfacial Transport and Form Rigid Interface for the Growth of Anchorage-Dependent Cells. *ACS Appl. Mater. Interfaces* **2014**, *6*, 21446–21453.
- (34) Gruner, P.; Riechers, B.; Semin, B.; Lim, J.; Johnston, A.; Short, K.; Baret, J. Controlling Molecular Transport in Minimal Emulsions. *Nat. Commun.* **2016**, *7*, 10392.
- (35) Courtois, F.; Olguin, L. F.; Whyte, G.; Theberge, A. B.; Huck, W. T. S.; Hollfelder, F.; Abell, C. Controlling the Retention of Small Molecules in Emulsion Microdroplets for Use in Cell-Based Assays. *Anal. Chem.* **2009**, *81*, 3008–3016.
- (36) Marcoux, P. R.; Dupoy, M.; Mathey, R.; Novelli-Rousseau, A.; Heran, V.; Morales, S.; Rivera, F.; Joly, P. L.; Moy, J. P.; Mallard, F. Micro-Confinement of Bacteria into W/o Emulsion Droplets for Rapid Detection and Enumeration. *Colloids Surfaces A Physicochem. Eng. Asp.* **2011**, *377* (1-3), 54–62.
- (37) Pan, M.; Lyu, F.; Tang, S. K. Y. Fluorinated Pickering Emulsions with Non-Adsorbing Interfaces for Droplet-Based Enzymatic Assays. *Anal. Chem.* **2015**, *87* (15), 7938–7943.
- (38) Davin-Regli, A.; Pages, J.-M. Enterobacter Aerogenes and Enterobacter Cloacae; Versatile Bacterial Pathogens Confronting Antibiotic Treatment. *Front. Microbiol.* **2015**, *6*, 392.
- (39) Kaminski, T. S.; Jakiela, S.; Czekańska, M. A.; Postek, W.; Garstecki, P. Automated Generation of Libraries of nL Droplets. *Lab Chip* **2012**, *12*, 3995–4002.
- (40) Chen, Y.; Gani, W. A.; Tang, S. K. Y. Characterization of Sensitivity and Specificity in Leaky Droplet-Based Assays. *Lab Chip* **2012**, *12*, 5093–5103.
- (41) Akobeng, A. K. Understanding Diagnostic Tests 3: Receiver Operating Characteristic Curves. *Acta Paediatr.* **2007**, *96* (5), 644–647.
- (42) Fawcett, T. An Introduction to ROC Analysis. *Pattern Recognit. Lett.* **2006**, *27* (8), 861–874.
- (43) Linnert, K. A Review on the Methodology for Assessing Diagnostic Tests. *Clin. Chem.* **1988**, *34* (7), 1379–1386.
- (44) Youden, W. J. Index for Rating Diagnostic Tests. *Cancer* **1950**, *3* (1), 32–35.
- (45) Hales, T. C. 1998 arXiv:math/9811071.
- (46) http://www.who.int/drugresistance/global_action_pl.
- (47) Akobeng, A. K. Understanding Diagnostic Tests 1: Sensitivity, Specificity and Predictive Values. *Acta Paediatr.* **2007**, *96* (3), 338–341.
- (48) Akobeng, A. K. Understanding Diagnostic Tests 2: Likelihood Ratios, Pre- and Post-Test Probabilities and Their Use in Clinical Practice. *Acta Paediatr.* **2007**, *96* (4), 487–491.
- (49) Debski, P. R.; Gewartowski, K.; Sulima, M.; Kaminski, T. S.; Garstecki, P. Rational Design of Digital Assays. *Anal. Chem.* **2015**, *87* (16), 8203–8209.
- (50) Lim, J.; Caen, O.; Vriignon, J.; Konrad, M.; Taly, V.; Baret, J.-C. Parallelized Ultra-High Throughput Microfluidic Emulsifier for Multiplex Kinetic Assays. *Biomicrofluidics* **2015**, *9* (3), 034101.
- (51) Kim, M.; Pan, M.; Gai, Y.; Pang, S.; Han, C.; Yang, C.; Tang, S. K. Y. Optofluidic Ultrahigh-Throughput Detection of Fluorescent Drops. *Lab Chip* **2015**, *15*, 1417–1423.
- (52) Holtze, C.; Rowat, A. C.; Agresti, J. J.; Hutchison, J. B.; Angilè, F. E.; Schmitz, C. H. J.; Köster, S.; Duan, H.; Humphry, K. J.; Scanga, R. A.; Johnson, J. S.; Pisignano, D.; Weitz, D. A. Biocompatible Surfactants for Water-in-Fluorocarbon



Table of Contents graphic

